5.3 RADIATION BIOLOGY

5.3.1 Studies on TLR agonist (MOS) Mediated Modification in Biological Radiation Response(s) *in vitro* after carbon beam exposure

Damodar Gupta[1], Sweta Sanguri[2]

[1]*Department of Capacity Enhancement and Product Induction, Institute of Nuclear Medicine and Allied Sciences, Defence Research and Development Organization, Timarpur, Delhi, India.*
[2]*Radiation Biology, Inter-University Accelerator Center, New Delhi, Delhi -110067*

To understand the health risk posed by ionizing radiation in accidental scenarios, patient undergoing radiotherapy, and in space exploration projects, the research needs to be directed in understanding molecular mechanism of damage, so that preventive or therapeutic measures can be adopted. To evaluate of the predictive radio-protective efficacy of MOS (a TLR agonist) along with possible mechanism of radiation protection after ^{12}C beam exposure. The study aims to understand the mechanistic aspects of radiation response in both radiation protection and radiation mitigation. The cells were irradiated with ^{12}C ion using the 15 UD Pelletron. ^{12}C ion with energy 85MeV (equivalent to 7.08 MeV/nucleon) from the accelerator.

Dose in Gray (Gy) was calculated from the particle fluence using the standard relation

Dose [Gy]=1.6×10^{-9}×LET [keV/µm] × Fluence [particles/cm^2]

The cells were exposed to C-ion beam, dose ranging 0 to 4 Gy.

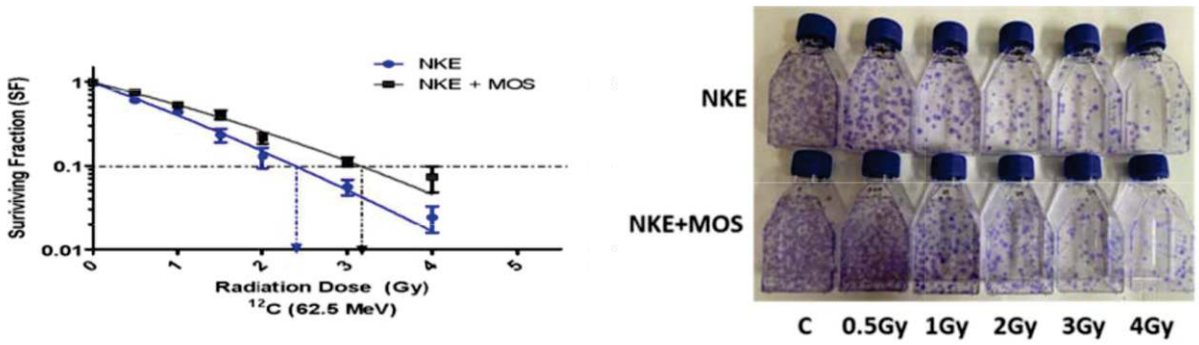

Fig 1(a): Clonogenic cell survival studies in NKE cells (normal kidney epithelial cells), irradiated with indicated doses of 12C beam with or without MOS pre-treatment. Cell cultures and treatments were performed identically and simultaneously in each experiment. Each data point is the mean of at least three individual experiments with similar results. Error bars represent standard deviations derived from six culture flasks. (b) Representative images of Clonogenic assay

The cell survival curves show surviving fraction after exposure to C ion beam in NKE cells (figure 1a)**.** NKE cells were exposed to ^{12}C ion beam and radiation modification effect of MOS pre-treatment was investigated. ^{12}C beams combined with MOS pre-treatment remarkably improved colony formation and cell survival in TLR expressing normal Kidney epithelial (NKE) cells. There was significant decrease in the MMP in NKE cells, 24 h post ^{12}C beam exposure probably due to damage and uncoupling of electron transport chain (ETC). Exposure to radiation compromises mitochondrial ETC function leading to mitochondrial dysfunctions (less ATP generation), alteration in calcium ion conc., increased oxidative stress (total and mitochondrial ROS/RNS) in cells as measured at 24 and 48 hours in NKE cells. MOS pre-treatment significantly amends all the perturbed above-mentioned parameters. Data will be communicated elsewhere soon. MOS, as a radiation countermeasure agent may also be beneficial in case of planned radiotherapy events in cancer patients, and may also provide health benefits for space crew by minimizing damage caused by cosmic radiation.

REFERENCES:

[1] Chang, D.S., Lasley, F.D., Das, I.J., Mendonca, M.S., Dynlacht, J.R. (2021). Stochastic, Deterministic, and Heritable Effects (and Some Radiation Protection Basics). In: Basic Radiotherapy Physics and Biology. Springer, Cham.

[2] Puspitasari, A.; Cerri, M.; Takahashi, A.; Yoshida, Y.; Hanamura, K.; Tinganelli, W. Hibernation as a Tool for Radiation Protection in Space Exploration. *Life*, **11**, 54(2021). https://doi.org/10.3390/life11010054

[3] Sanguri, S., Gupta, D. Mannan oligosaccharide requires functional ETC and TLR for biological radiation protection to normal cells. BMC Cell Biol **19**, 9 (2018). https://doi.org/10.1186/s12860-018-0161-4

5.3.2 Lithium Chloride enhances survival of INT407 cells in response to High Linear Energy Transfer Radiation

Mitu Lal,Asitikantha Sarma

Inter University Accelerator Centre (IUAC), Aruna Asafali Marg, New Delhi-110067, India

The autophagy process is important in the removal of damaged cell organelles following radiation interaction. Modulation of autophagy and the related mechanisms by High LET radiation is a less explored area of research; hence a thorough study in this direction is required. The aim of the present study was to investigate the effect and mechanism of the synergistic killing cells induced by high LET radiation in combination with autophagy drugs. The energy of carbon ion beam on the cell surface was 62 MeV (equivalent 5.16 MeV/nucleon). Human embryonic intestinal cells (INT407 cells) were irradiated with 1Gy radiation. The cells were treated with autophagy inducers chloroquine (CQ), ammonium chloride (NH_4CL) and autophagy blocker lithium chloride (LiCl). Cellular cytotoxicity and cell proliferation was assessed by MTT and SRB-uptake assay.

Induction of autophagy was examined by staining cells with monodansylcadaverine (MDC) and western blot for studying expression of autophagy related gene (ATG). Cell proliferation assay showed decline in cell proliferation in INT407 cells exposed to CQ (20µM) and NH_4Cl (20mM) in combination with radiation (1Gy). However, pretreatment of cells with LiCl (20mM) was found to be protective and augmented cell proliferation (72hr). The MDC dye was used to assess levels of mature autophagic vesicle formation following radiation. The current study offers strong evidence that LiCl (20mM) pretreatment has ability to prevent cells from autophagic cell death in response to carbon ion beam radiation in INT407 cells. Lithium chloride combined with radiation increased the duration of survival of cells. However, LiCl treatment could be effective for the medical treatment of colon cancers. LiCl can be used as radio protective agent against autophagy as it enhances survival after exposure to ^{12}C radiation in human intestinal cells.

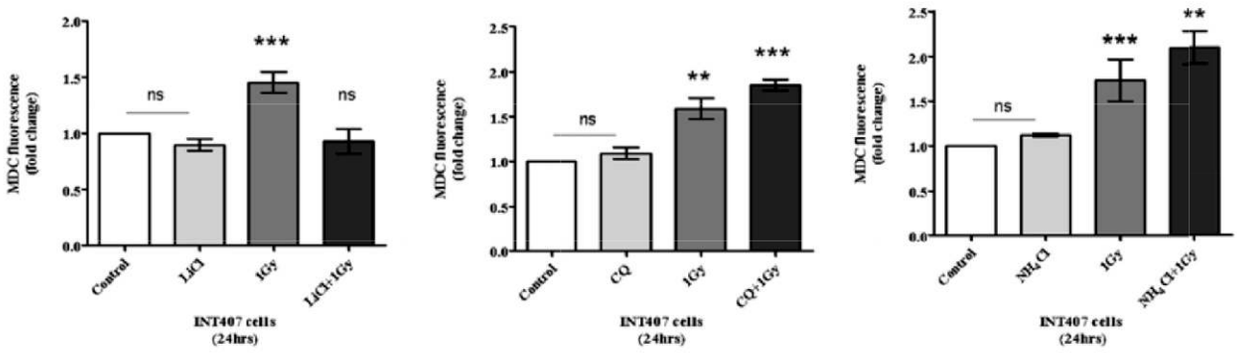

Figure 1: Detection of lysosomal activity in live cells. INT407 cells were treated with lysomotropic agents (CQ, NH_4Cl and LiCl) and exposed to radiation ^{12}C (1Gy). MDC positive autophagosomes accumulated after radiation treatment (24hr). MDC marks autophagic compartments after their fusion to acidic endo/lysosomes. Quantification of the MDC fluorescence assay results from (a-c) are shown in the bar graph, Results were expressed as Mean ± SD. n = 3 (* p < 0 .05; **p < 0.01, *** p<0.001) one way ANOVA.

Autophagy is a catabolic process that protects cells from a wide variety of stresses, such as nutrient starvation, organelle damage, and protein aggregation [1]. Autophagy is a balance that weights between reconstruction, energy equilibrium, cell death and survival, correspondingly, with the internal or external stimulations accepted [2].

We used monodansylcadaverine (MDC), a specific autophagolysosome marker to analyze at the molecular level the machinery involved in the autophagic process. With this assay we observed that the accumulation of MDC was specifically induced by radiation 1Gy. Additionally, lithium chloride (20mM) an autophagy blocker blocks autophagy at 24hrs (fig a), inhibited the accumulation of MDC in autophagic vacuoles. Conversely, CQ and NH4Cl increased the accumulation of MDC (fig b,c) and altered the distribution and size of the autophagic vacuoles.

REFERENCES:

[1] Li X, He S, Ma B. Mol Cancer **19**(1):12(2020)

[2] Wu WKK, Coffelt SB, Cho CH, Wang XJ, Lee CW, Chan FKL, et al. Oncogene. **31** (8):939–53(2012)

5.3.3 Cellular response to high LET radiation exposure with special reference to mitochondria

Sweta Sanguri, Asitikantha Sarma

Radiation Biology, Inter-University Accelerator Centre, New Delhi, Delhi -110067

High-LET radiation creates more complex and diverse cellular effects; however, the fundamental molecular mechanisms of high-LET radiation-induced cellular cytotoxicity continue to be a matter of investigation. Mitochondria, being the power-house of the cell, are one of the most important targets of radiation because they are the site of oxidative phosphorylation, where energy production (ATP) occurs by utilizing molecular oxygen, which further increase the oxidative stress. The current study aims to determine the effects of carbon ion beam on mitochondrial fission-fusion homeostasis and ETC function.

The energy of carbon ion beam on the cell surface was 62 MeV (equivalent 5.16 MeV/nucleon). The irradiation dose range used was from 0 to 4 Gy.

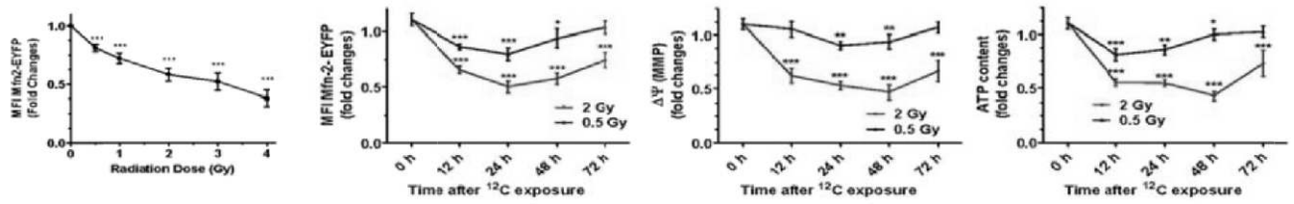

*Fig 1(a): Changes in mean fluorescence intensity (MFI) of HEK 293T cells expressing Mfn2-EYFP protein 12 hours post exposure to 12C beam (b) MFI of Mfn2-EYFP protein at indicated doses and time points. Image acquisition was done using ZOE™ Fluorescent Cell Imager (BioRad, USA). Data was analysed using Image J software for macOSX. Results are expressed as MFI (fold changes) with respect to control ± SD. (c) Mitochondrial Membrane Potential by staining cells with DiOC6(3) and (d) Cellular ATP content was measured using luminescent ATP measurement kit, measured using multimode plate reader at indicated doses and time points. Differences were designated significant at values * $p < 0$.*

Expectedly, alteration in mitochondrial structure and dynamics increases with increasing radiation dose. Results *(figure 1)* illustrate decrease in mean fluorescence associated with Mfn2 protein 12 hrs post ^{12}C beam exposure in comparison to sham irradiated control cell. The time kinetics study shows further drop in MFI at 24 h post exposure in both the doses, and MFI starts to improve by 48 h and reverts back to basal level in 0.5 Gy exposed cells. MFI appeared to improve in 2 Gy irradiated cells but the basal MFI was never achieved in even the later time points. Initial drop in Mfn2 associated fluorescence signify shift towards mitochondrial fission and consequently a greater number of mitochondria per cell.

To maintain cellular bioenergetic status, the cells need a greater number of mitochondria resulting in more mitochondria fission events. The present study demonstrates that mitochondrial health is vital for the structural integrity and normal cellular function. ^{12}C beam exposure in NKE created a major energy crisis, accompanied by increase in mitochondrial mass, and respiration (data not shown). Carbon ion exposure created a major energy crisis in normal cells, as reflected by the low ATP yield and the alterations in bioenergetic-related SU9 protein (shown earlier). Decrease in cellular ATP and ΔΨm levels signals cell to increase ETC function to cope up with the energy demands and also maintain falling MMP levels as indicated by increased expression of Su9 protein (of complex V) of ETC. To maintain cellular bioenergetic status cells need a greater number of mitochondria (more mitochondria fission) and more ETC machinery (more electron transport chain function to produce more ATP). Low dose exposure to ^{12}C beam caused a transient perturbation in mitochondrial physiology and function and the cells recovered from the low dose insult by 72 h. Alteration in mitochondrial dynamics and ETC function caused by exposure to higher dose of ^{12}C irreversibly affects physiological and metabolic state of normal cells at doses higher than 0.5 Gy.

REFERENCES:

1. Westermann, B., Mitochondrial fusion and fission in cell life and death. Nat Rev Mol Cell Biol, **11**(12): p. 872-84(2010).
2. Averbeck, D.; Rodriguez-Lafrasse, C. Role of Mitochondria in Radiation Responses: Epigenetic, Metabolic, and Signaling Impacts. Int. J. Mol. Sci., **22**, 11047(2021). https://doi.org/10.3390/ijms222011047

5.3.4 Study of DNA damage response pathway of A549 cells treated with carbon ion in presence of PARP-1 inhibitor

Dey Payel[a], Ghosh Sourav[a], Sarma Asitikantha[c], Ghosh Utpal[a*]

a Department Of Biochemistry & Biophysics, University of Kalyani, Kalyani, Nadia, West Bengal, PIN- 741235
b Inter-University Accelerator Center, New Delhi, Delhi -110067

Lung cancer is the most commonly diagnosed malignancy worldwide. Although ionizing radiation is widely established standard radiotherapy against lung cancer, but variety of reports shows the rise of malignant traits after radiotherapy. However, these limitations are overcome in hadrons therapy especially using carbon ion which has been established as a promising modality to treat cancer. In DNA Damage Response (DDR) pathway, a number of signaling molecules get activated after DNA damage to arrest the cell cycle and attempt to repair the DNA. DDR is an intricate kinase-based signaling pathway, which senses, transduces, and exerts a strong effect on any DNA lesions [1]. In the case of high-LET irradiation, more than 90% of DSBs are related to clustered lesions. Higher eukaryotes possess several principal repair pathways to recover DSBs, namely non-homologous end-joining (NHEJ), homologous recombination (HR), single-strand annealing (SSA), and at least two alternative end-joining mechanisms [2]. PARP-1 acts as a potent sensor for DNA damage that produces PAR at newly generated DNA DSBs rapidly and promotes the recruitment of repair factors. Notably, PARP-1 inhibition causes tumor-specific synthetic lethality by repressing the single-strand break (SSB) repair, base excision repair (BER), and alternative non-homologous end joining (Alt-NHEJ) [3]. Unfortunately, DSBs caused by PARP-1 inhibitor are often repaired by homologous recombination. Thus, PARP inhibitors including Rucaparib, Niraparib, Olaparib are approved by

FDA for the therapy of BRCA1/2-mutant ovarian cancer and breast cancer whose HR capability is compromise. Recently, PARP-1/2 inhibitors were used to treat a variety of human cancers including brain, lung, and cervical carcinomas. The role of PARP-1 in cluster DNA damage is largely unknown. Our aim was to investigate role of PARP-1 in DNA repair after cluster DNA damage. We checked DNA damage by measuring Gamma H2AX foci in a time-dependent manner after treatment with ^{12}C-ion and olaparib (PARP-1 inhibitor). The data is shown in Fig 1 &2.

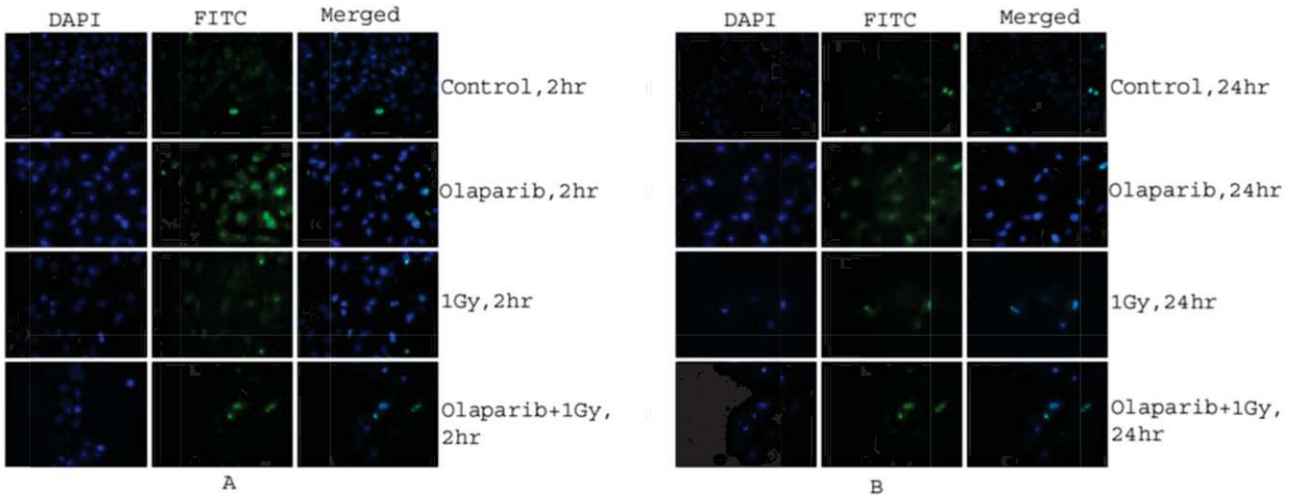

Fig 1: DNA breaks as detected by γ-H2AX foci in A549 cells exposed with ^{12}C ion in presence or absence of PARP-1 inhibitor olaparib (1μM) for (1A) 2hr and (1B) 24hr.

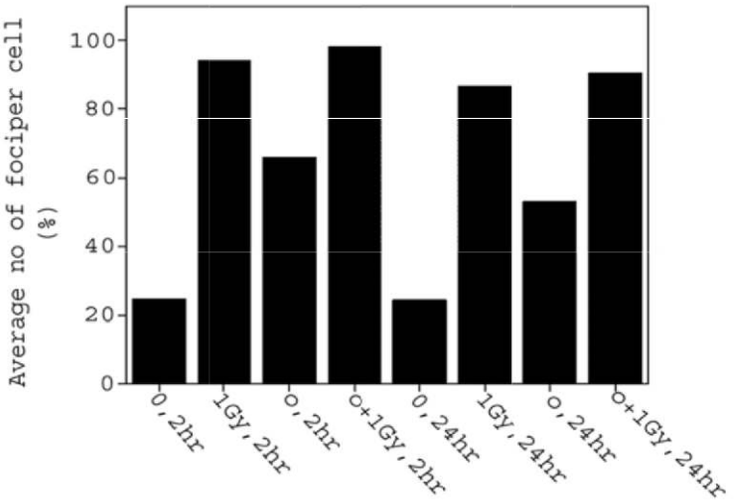

Fig 2: Plot of average no of Gamma H2AX foci per cell with respect to ^{12}C ion in presence and absence of PARP-1 inhibitor Olaparib for 2hr and 24hr.

REFERENCES:

[1] Gerelchuluun A, Manabe E, Ishikawa T, Sun L, Itoh K, Sakae T, *et al* Radiat Res [Internet]. 2015 Mar 1 [cited 2021 Dec 11];**183**(3):345–56.

[2] Natale F, Rapp A, Yu W, Maiser A, Harz H, Scholl A, *et al.* Nat Commun [Internet]. 2017 Jun 12 [cited 2021 Dec 12];8.

[3] Metzger MJ, Stoddard BL, Monnat RJ. DNA Repair (Amst) [Internet]. 2013 Jul [cited 2021 Dec 11];**12**(7):529–34.

5.4 ACCELERATOR MASS SPECTROMETRY AND GEOCHRONOLOGY

5.4.1 Radiocarbon Dating for determining sedimentation rate and associated palaeoclimate from the Kolahoi Glacier outwash plain

Rayees Ahmad Shah[1, 2] Mohammad Saleem[1] and Shakil Ahmad Romshoo[1, 2]

[1]*Department of Geoinformatics, Centre of Excellence in Glacier studies, University of Kashmir, Hazratbal Srinagar, 190006, India*

[2]*DCentre for Science and Society, Islamic University of Science and Technology (IUST), Awantipora, Kashmir 192123, India*

A comprehensive fieldwork of 10 days was carried at Kolahoi Glacier during in June 2021 to investigate sediment sequence deposited in front of the Kolahoi Glacier. The objective of the study was to determine the sedimentation rate of the outwash plain in order to reconstruct palaeoclimate of the Kolahoi Glacier valley which has shown

significant deglaciation in the Holocene [*for details, see J. of Asian Earth Sciences, 138 (2017) 38–50*]. A 177 cm long section was excavated near the outwash plain of the Kolahoi Glacier and a total of 59 sediment samples were collected at 3 cm interval. An alternate coarse and fine-grained sediments were observed in the excavated sediment section. The sampled sediments represent a dynamic hydrological regime that transported the sediments. The following samples (Table 1) collected from Kolahoi Glacier were analyzed at IUAC New Delhi for Radiocarbon ages. However, the data does not reveal ages in stratigraphic order and thus needs to be further investigated. The AMS age of the sample 9, that was the only intact wood piece retrieved from the sediment sequence, has been revealed as expected.

Table 1: AMS Radiocarbon ages of the samples analyzed at IUAC

S. No.	Sample Name	Depth	Sample ID	pMC value	Radiocarbon Age (BP)	Comment
1.	Sample_1	2 cm	IUACD#21C3957	101.027 ± 0.264	-82 ± 21	Modern
2.	Sample_2	17 cm	IUACD#21C3958	43.356 ± 0.148	6713 ± 27	
3.	Sample_3	39 cm	IUACD#21C3959	84.078 ± 0.229	1393 ± 21	
4.	Sample_4	70 cm	IUACD#21C3960	84.919 ± 0.234	1313 ± 22	
5.	Sample_5	80 cm	IUACD#21C3961	76.040 ± 0.210	2200 ± 22	
6.	Sample_6	128 cm	IUACD#21C3962	36.699 ± 0.132	8052 ± 28	
7.	Sample_7	140 cm	IUACD#21C3963	58.119 ± 0.173	4359 ± 23	
8.	Sample_8	173 cm	IUACD#21C3964	57.608 ± 0.172	4430 ± 23	
9.	Sample_9	176 cm	IUACD#21C3965	82.561± 0.222	1539 ± 21	

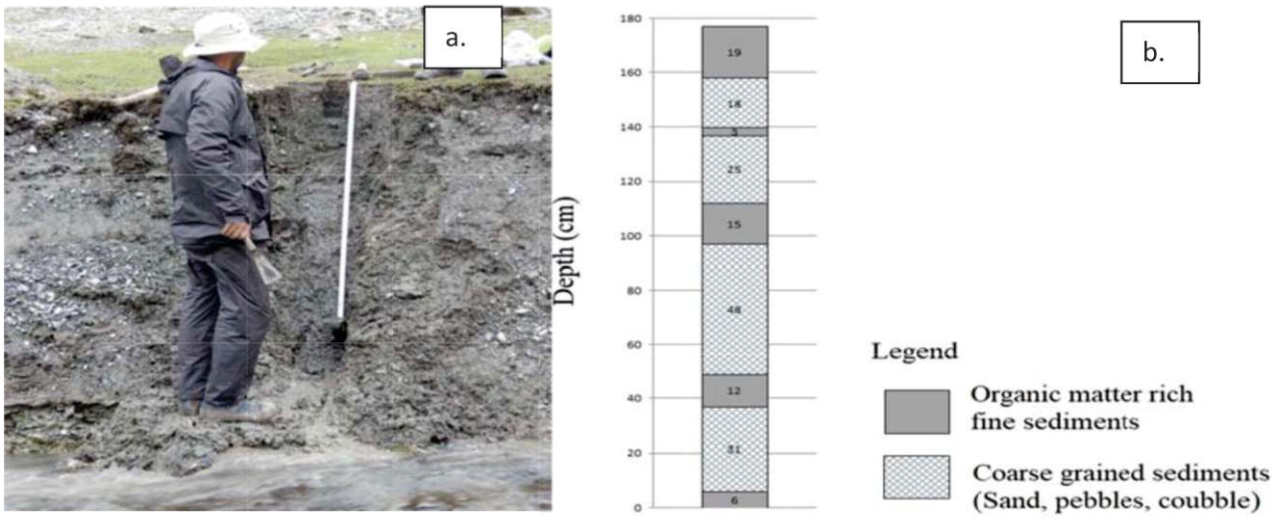

Figure 1: (a) Photograph of the Kolahoi glacier outwash plain section
(b.) Litholog of the outwash plain section

REFERENCES:

[1] Irfan Rashid, Shakil Ahmad Romshoo, and Tariq Abdullah. Journal of Asian Earth Sciences, **138**, 38–50(2017)

5.4.2 Investigating the radiocarbon chronology of wetland sediment cores from Kashmir Himalaya

Shahid Ahmad Dar[1], Sami Ullah Bhat[1], Irfan Rashidl[2], Pankaj Kumar[3] and Rajveer Sharma[3]

[1]*Department of Environmental Science, University of Kashmir, India*

[2]*Department of Geoinformatics, University of Kashmir, India.*

[3]*Inter University Accelerator Centre, New Delhi, India*

In order to investigate the ages of the sediment samples, sediment cores were collected from two wetland sites in Kashmir Himalaya. A UWITEC gravity-corer fitted with a poly-vinyl chloride (PVC) pipe having a diameter of 63 mm was used for the collection of the sediment cores. Sampling was carried out below 2 feet water depth. The sediment cores were subsampled at a regular interval of 2 cm resolution. Before analysis, the samples were dried, powdered, and removed of any extraneous material. A total of 8 carbon rich samples were selected for ^{14}C dating.

The analysis was performed using the accelerator mass spectrometry (AMS) facility at the Inter-University Accelerator Centre (IUAC), New Delhi, India. The sediment samples were first cleaned physically to remove visible contaminations. After that, the samples were exposed to acid-base-acid (HCl-NaOH-HCl) treatment following the standard methodology [1]. After each step of solvent treatment, the samples were rinsed with deionized water. ABA treated samples were freeze-dried for about 10 h. The freeze-dried sample was wrapped in the tin boats and burnt under a controlled atmosphere at 920˚C. The produced carbon dioxide gas was purified and mixed with hydrogen and reduced to graphite in presence of iron powder (catalyst) using automated graphitization equipment (AGE) [2]. Resultant graphite was loaded in the ion source of AMS for radiocarbon measurement. All the ^{14}C ages were calibrated using the online OxCal program (OxCal v4.4.4) using the Northern Hemisphere terrestrial curve IntCal20 [3]. The Accelerator Mass Spectrometer (AMS) assisted ^{14}C dating of the sediment core showed ^{14}C age reversals for the one wetland site while a linear increase in the age of the samples with depth was observed for another wetland site.

REFERENCES:

[1] Sharma, R., Umapathy, G. R., Kumar, P., Ojha, S., Gargari, S., Joshi, R., ... & Kanjilal, D. (2019). Ams and upcoming geochronology facility at inter university accelerator centre (IUAC), New Delhi, India. Nuclear Instruments and Methods in Physics Research Section B: Beam Interactions with Materials and Atoms**, 438,** 124-130. doi: 10.1016/j.nimb.2018.07.002

[2] Wacker, L., Němec, M., & Bourquin, J. (2010). A revolutionary graphitisation system: fully automated, compact and simple. Nuclear Instruments and Methods in Physics Research Section B: Beam Interactions with Materials and Atoms, **268**(7-8), 931-934.

[3] Reimer, P. J., Austin, W. E., Bard, E., Bayliss, A., Blackwell, P. G., Ramsey, C. B., ... & Talamo, S. (2020). The IntCal20 Northern Hemisphere radiocarbon age calibration curve (0–55 cal kBP). Radiocarbon, **62**(4), 725-757.

5.4.3 Ventilation of Northern Indian Ocean during the last glacial-interglacial cycle

Kumari Nisha[1,2*], Sushant Suresh Naik[1], Pankaj Kumar[3]

[1]*CSIR-National Institute of Oceanography, Dona-Paula, Goa, India*
[2]*School of Earth, Ocean and Atmospheric Sciences, Goa University, Goa, India*
[3]*Inter-University Accelerator Centre (IUAC), New Delhi, India*

In order to reconstruct the ventilation age changes in the northern Indian Ocean for the last glacial-interglacial cycle, AMS radiocarbon dating of foraminifera from a gravity core AAS-9/21 (1807 m water depth) collected from the Eastern Arabian Sea (EAS) was carried out at the Inter-University Accelerator Centre (IUAC), India. Here the ventilation ages of the intermediate water are reported as the radiocarbon age difference between paired bottom water-dwelling benthic foraminifera and surface-dwelling planktic foraminifera (B-P), based on Broecker *et al*., 1984, which represents deep-surface radiocarbon age offset. In order to cover the objectives of this research, samples from specific intervals like the Last Glacial Maximum (LGM), Heinrich Stadial (HS), Bolling-Allerod (B-A), Younger Dryas (YD) and Holocene were used. Fifteen radiocarbon dates from the core AAS-9/21 were obtained using 9 samples of mixed-species of benthic foraminifera (excluding pyrgo and agglutinated species) and 6 coexisting mono-species planktic foraminifera (*Globigerinoides ruber*). To carry out AMS radiocarbon dating, at least 13mg of each, planktic and benthic foraminifera from a size fraction of >250 µm were identified and picked using stereo-200m binocular microscope (Meiji Techno EMZ-5). In some benthic samples, weights were less than 13 mg, in such samples mixed benthic foraminifera (size fraction >250 µm) from the previous interval were added. The radiocarbon dates were calibrated to calendar ages by using Calib 8.20 software (Stuiver & Reimer, 1993). The concentration of radiocarbon in ocean and atmosphere differs, hence, Marine20 calibration curve (Heaton, *et al.*, 2020) is used and corrected with reservoir age correction of ΔR 4 ± 62years (Dutta, *et al*., 2001; Southon, *et al*., 2002). x

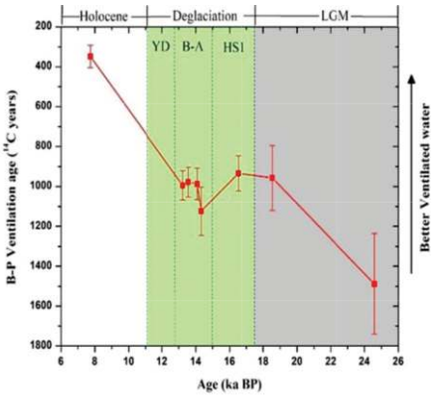

Figure 1: Ventilation age record for the core AAS-9/21

The reconstructed benthic-planktic (B-P) ventilation ages for the eastern Arabian Sea intermediate water suggest that there have been significant changes during the last 25kyr. The apparent age difference between coexisting benthic and planktic during the LGM was ~1500 ^{14}C years

suggesting existence of poorly ventilated water in the EAS. Ventilation age decreased during the early deglaciation. The benthic-planktic age offset reached up to ~900 ^{14}C years indicating an inflow of better-ventilated water at the core site. The ventilation age fluctuated between ~200 ^{14}C years through the deglaciation. The ventilation age significantly decreased during the Holocene as low as ~400 years indicating intensified penetration of better-ventilated water into the EAS.

REFERENCES:

[1] Broecker, W., Mix, A., Andree, M., Oeschger, H., 1984. Radiocarbon measurements on coexisting benthic and planktic foraminifera shells: potential for reconstructing ocean ventilation times over the past 20 000 years. Nuclear Instruments and Methods in Physics Research Section B: Beam Interactions with Materials and Atoms, **5**(2), 331-339.

[2] Dutta, K., Bhushan, R., Somayajulu, B., 2001. ΔR correction values for the northern Indian Ocean. Radiocarbon, **43**(2A), 483-488.

[3] Heaton, T.J., Köhler, P., Butzin, M., Bard, E., Reimer, R.W., Austin, W.E., Ramsey, C.B., Grootes, P.M., Hughen, K.A., Kromer, B., Reimer, P.J., 2020. Marine20—the marine radiocarbon age calibration curve (0–55,000 cal BP). Radiocarbon, **62**(4),779-820.

[4] Southon, J., Kashgarian, M., Fontugne, M., Metivier, B., Yim, W.W., 2002. Marine reservoir corrections for the Indian Ocean and Southeast Asia. Radiocarbon, **44**(1), 167-180.

[5] Stuiver, M., Reimer, P.J., 1993. Extended 14C data base and revised CALIB 3.0 14C age calibration program. Radiocarbon, **35**(1), 215-230.

5.4.4 ^{14}C dating of Ground Water from Malwa Region of Punjab State using Accelerator Mass Spectrometry (AMS)

A. Srivastava[1,*], N. Chauhan[1], S. Chopra[2], Pankaj Kumar[2], R. Sharma[2], P.V. Kumar[2], Meenakshi[2] and R. Patnaik[3]

[1]Department of Chemistry, Panjab University Chandigarh, India

[2]Inter-University Accelerator Centre (*IUAC*), New Delhi, India

[3]Department of Geology, Panjab University Chandigarh, India

The Malwa region of Punjab is known to have elevated level of uranium in its ground water. A number of studies have been carried out to determine the source of uranium in the ground water of the above mentioned region. Two hypotheses have been proposed namely anthropogenic and geogenic based on the data so far collected [1,2,3]. In the reported work 11 ground water samples from different locations and depths respectively were collected and their ^{14}C based age was determined using Accelerator Mass Spectrometry (AMS). The underlying hypothesis being that age of groundwater has direct dependence with the nature of source.

Table 1. **Radiocarbon age of ground water samples in year before present (BP)**

Sample ID	Depth (feet)	*Radiocarbon Age (BP) in years*
A-19	40	370
A-18	40	1461
A-21	100	272
A-20	100	1065
A-7	350	7292
A-10	400	524
A-8	400	2838
A-12	450	3126
A-4	550	5001
A-6	600	13448
A-1	700	8806

It is observed from Table 1 that the age value of ground water collected from different depths and locations from the affected region ranges between 272 years before present (BP) and 13448 years before present (BP). The preliminary work carried out indicates that the age of ground water irrespective of location or depth is older than the advent of industrial revolution. It is important to note here that it was only after the industrial revolution that anthropogenic pollution became really significant. It is therefore argued that the presence of uranium in ground water perhaps could be of geogenic origin as anthropogenic input due to modern farm practices which could have added uranium

to the local ground water source from phosphate based fertilizers, pesticides, fly ash leachants and irrigation with water enriched with domestic/ industrial effluents etc. were nonexistent during the period of time indicated in the present work. It would be interesting to carry out a more focused study to get a clearer picture since the data base is rather small and scanty.

REFERENCES:

[1] E. Schnug, B. G. Lottermoser, Environ. Sci. Technol. Lett., **47**, 6, 2433–2434(2013).

[2] A. Srivastava, V. Chahar, V. Sharma, Y. Sun, R. Bol, F. Knolle, E. Schnug, F. Hoyler, N. Naskar, S. Lahiri, R. Patnaik, J. Radioanal. Nucl. Chem., **314**, 1367–1373(2017).

[3] R. M. Coyte, R. C. Jain, S. K. Srivastava, K. C. Sharma, A.Khalil, Lin Ma, and A. Vengosh, Environ. Sci. Technol. Lett., **5**, 6 ,341–347(2018).

5.4.5 Study of role of nitrate in determination of elemental concentration of heavy elements in ground water using Inductively Coupled Plasma Mass Spectrometry (ICP-MS)

P.V. Kumar[1], N. Chauhan[2], V. Chahar[2], M.Maekawa[3], S. Chopra[1], E.W.Schnug[3], R. Patnaik[4] and A Srivastava[2*]

[1]Inter-University Accelerator Centre (*IUAC*), New Delhi, India

[2]Department of Chemistry, Panjab University Chandigarh, India

[3]Institute of Soil and Plant Science, Julius Kuehn Institute, Braunschweig, Germany

[4]Department of Geology, Panjab University Chandigarh, India

It is well known that ground water samples need to be acidified by ultra pure nitric acid to keep heavy elements in dissolved state (1) to avoid underestimation of their concentration as the elements are prone to adhere to the wall of the container with passage of time. In the present work the leaching behavior of different elements from the wall of the container used for study of ground water of Malwa region known to have elevated level of uranium (2,3) was studied as a function of time to understand the role of nitrate in mobilization of elements.

Table 1. **Concentration of different heavy elements in ground water samples without and with acidification**

ID	**Concentration of elements without acidification**							**Concentration of elements with acidification**						
	Mg ppm	K ppm	Ca ppm	Fe ppb	U ppb	As ppb	Sr ppm	Mg ppm	K ppm	Ca ppm	Fe ppb	U	As ppb	Sr ppm
A-1	33.83	3.44	7.80	7.42	0.04	1.45	1.37	44.6	11.1	84.3	14.1	7.54	2.21	2.62
A-4	9.26	2.26	1.57	1.13	7.30	4.02	0.37	10	5.35	<6.3	11	34	3.95	0.51
A-6	11.04	2.19	2.01	0.30	6.85	4.92	0.34	13.9	3.79	<6.3	15.4	36.1	5.25	0.65
A-7	12.34	1.65	1.87	1.16	15.08	2.11	0.51	14.3	4.77	<6.3	5.07	87.5	2.77	0.76
A-8	3.91	0.93	0.93	BDL	5.51	3.53	0.29	4.01	2.6	<6.3	4.60	46.1	3.53	0.24
A-10	35.45	3.22	4.95	1.60	28.33	1.25	0.61	45.9	10.3	60.7	4.31	52.4	1.35	1.05
A-12	20.27	3.30	2.43	1.60	8.91	1.98	0.51	24.1	5.93	<6.3	8.6	40.7	2.14	0.74
A-18	93.01	12.6	20.91	11.17	25.48	0.65	8.67	121	48.4	175	4.91	64.6	0.36	14.6
A-19	122.4	7.48	19.23	13.91	5.43	0.67	3.37	168	21.6	286	5.20	17.8	0.40	5.39
A-20	22.54	3.00	3.12	0.19	17.20	3.31	0.73	36.3	8.08	10.4	8.40	44.7	4.09	1.57
A-21	58.96	2.23	8.79	5.18	41.68	0.73	0.73	96.1	11.6	190	6.47	76.7	0.21	2.77

The concentration of seven elements namely Mg, K, Ca, Fe, U, As and Sr were determined with and without acidification with nitric acid. It was observed that concentration of Mg, Sr and As were not significantly influenced by nitrate acidification but the concentration of K, Ca, Fe and U were affected in a significant manner with Uranium being the most significant. The leaching behavior study which was later carried out showed that addition of nitric acid to the non acidified samples resulted in the concentration of elements therein specially those which were significantly affected become comparable to those in acidified samples in three weeks time.

REFERENCES:

[1] J. Nolan and K. A. Weber; Sci. Technol. Lett., **2** , 215−220(2015).

[2] B.S.Bajwa, S. Kumar, S. Singh, S.K.Sahoo, R.M.Tripathi: J. Radia. Resear. Appl.Sci. **10** (2017)13-19(2017).